Synthesis and Electroluminescence Properties of Novel Main Chain Poly(*p*-phenylenevinylene)s Possessing Pendant Phenylazomethine Dendrons as Metal Ligation Sites

Atsushi Kimoto, Kiriko Masachika, Jun-Sang Cho, Masayoshi Higuchi, and Kimihisa Yamamoto*

Kanagawa Academy of Science & Technology (KAST), Department of Chemistry, Faculty of Science and Technology, Keio University, Yokohama 223-8522, Japan

Received May 14, 2004. Revised Manuscript Received September 21, 2004

Novel poly(*p*-phenylenevinylene)s with a dendritic phenylazomethine (DPA-PPVs) were synthesized via the Heck reaction by initially complexing with rare-earth-metal ions, by filling up the coordination trap site of dendritic phenylazomethine (DPA) as the catalyst. The physical properties of the DPA-PPVs were evaluated. The solution, thermal, and optical properties affected by the various contents and generation of the DPA were investigated. DPA-PPV with the lower content and a smaller generation number showed the longest absorption and fluorescence maximum wavelength based on a relatively planar structure and a longer conjugation length. These polymers successfully assemble metal ions on their imine site supported by the spectral change similar to their monomeric model compounds. Two types of electroluminescent (EL) devices were fabricated: (I) ITO/PEDOT/DPA-PPV/Alq/CsF/Al; (II) ITO/PEDOT/DPA-PPV/TAZ/Alq/CsF/Al, where Alq (tris-8-hydroxyquinoline aluminum) acts as an electron transport layer (ETL) and TAZ (3,5-bis(*tert*-butylphenyl)-4-phenyltriazole) acts as a hole-blocking layer. In both devices, the luminescence from DPA-PPV was observed with a lower generation and a smaller amount of the DPA unit (**3a**), as explained by its physical properties. For the type II device with **3a**, the emission from DPA-PPV, the lower driving voltage and enhanced efficiency were followed by simply complexing with a very small amount of $SnCl_2$. On the other hand, for **3b**, the emission from Alq, not from DPA-PPV, was enhanced by the complexation, and **3b**-$SnCl_2$ mainly acts as a hole transport layer with the enhanced hole injection and recombination into the Alq layer, which could not be completely blocked because of the enhanced hole transport property of the DPA unit.

Introduction

Functional π-conjugated polymers have inspired various applications such as organic light-emitting diodes (OLEDs)[1] and photocells.[2] Recently, various substituents on the PPVs have been introduced, providing additional properties and performing as magnetic,[3] charge-transporting,[4] and sterically hindered to prevent interchain interactions and a self-quenching process of excitons.[5]

Recently, we reported hole transport materials with a phenylazomethine moiety as a metal-collecting unit that resulted in a higher EL efficiency only by complexation with a metal ion.[6] Toward the emitting material in OLEDs, we have synthesized novel poly(*p*-phenylenevinylene)s (DPA-PPVs) with a phenylazomethine dendron as a metal-collecting site.

In general, two different synthetic routes can be applied to yield dendron-functionalized main chain polymers also referred to as linear dendritic, architectural copolymers.[7] The first route utilizes a polymer backbone

* Author to whom correspondence should be addressed. E-mail: yamamoto@chem.keio.ac.jp.

(1) (a) Burroughes, J. H.; Bradley, D. D. C.; Brown, A. R.; Marks, R. N.; MacKay, K.; Friend, R. H.; Burn, P. L.; Holmes, A. B. *Nature* **1990**, *347*, 539. (b) Greenham, N. C.; Moratti, S. C.; Bradley, D. D. C.; Friend, R. H.; Holmes, A. B. *Nature* **1993**, *365*, 628. (c) Tessler, N.; Denton, G. J.; Friend, R. H. *Nature* **1996**, *382*, 695. (d) Welter, S.; Brunner, K.; Hofstraat, J. W.; De Cola, L. *Nature* **2003**, *421*, 54.

(2) (a) Yu, G.; Gao, J.; Hummelen, J. C.; Wudl, F.; Heeger, A. J. *Science* **1995**, *270*, 1789. (b) van Hal, P. A.; Wienk, M. M.; Kroon, J. M.; Verhees, W. J. H.; Slooff, L. H.; van Gennip, W. J. H.; Jonkheijm, P.; Janssen, R. A. J. *Adv. Mater.* **2003**, *15*, 118. (c) Ago, H.; Petritsch, K.; Shaffer, M. S. P.; Windle, A. H.; Friend, R. H. *Adv. Mater.* **1999**, *11*, 1281. (d) Stalmach, U.; de Boer, B.; Videlot, C.; van Hutten, P. F.; Hadziioannou, G. *J. Am. Chem. Soc.* **2000**, *122*, 5464.

(3) (a) Nishide, H.; Kaneko, T.; Nii, T.; Katoh, K.; Tsuchida, E.; Yamaguchi, K. *J. Am. Chem. Soc.* **1995**, *117*, 548. (b) Nishide, H.; Kaneko, T.; Nii, T.; Katoh, K.; Tsuchida, E.; Lahti, P. M. *J. Am. Chem. Soc.* **1996**, *118*, 9695.

(4) (a) Lee, Y.-Z.; Chen, X.; Chen, S.-A.; Wei, P.-K.; Fann, W.-S. *J. Am. Chem. Soc.* **2001**, *123*, 2296. (b) Pu, Y.-J.; Soma, M.; Kido, J.; Nishide, H. *Chem. Mater.* **2001**, *13*, 3817. (c) Li, H.; Hu, H.; Zhang, Y.; Ma, D.; Wang, L.; Jing, X.; Wang, F. *Chem. Mater.* **2002**, *14*, 4484. (d) Kim, J. H.; Park, J. H.; Lee, H. *Chem. Mater.* **2003**, *15*, 3414.

(5) (a) Bao, Z.; Amundson, K. R.; Lovinger, A. J. *Macromolecules* **1998**, *31*, 8647. (b) Sohn, B.-H.; Kim, K.; Choi, D. S.; Kim, Y. K.; Jeoung, S. C.; Jin, J.-I. *Macromolecules* **2002**, *35*, 2876. (c) Shin, D.-C.; Kim, Y.-H.; You, H.; Kwon, S.-K. *Macromolecules* **2003**, *36*, 3222. (d) Mikroyannidis, J. A. *Chem, Mater.* **2003**, *15*, 1865.

(6) (a) Sato, N.; Cho, J.-S.; Higuchi, M.; Yamamoto, K. *J. Am. Chem. Soc.* **2003**, *125*, 8104. (b) Kimoto, A.; Cho, J.-S.; Yamamoto, K. *J. Photopolym. Sci. Technol.* **2003**, *16*, 293. (c) Cho, J.-S.; Kimoto, A.; Nishiumi, T.; Yamamoto, K. *J. Photopolym. Sci. Technol.* **2003**, *16*, 295. (d) Kimoto, A.; Cho, J.-S.; Higuchi, M.; Yamamoto, K. *Macromolecules* **2004**, *37*, 5531.

10.1021/cm049241m CCC: $27.50
Published on Web 11/18/2004

with anchor groups to either convergently or divergently attach a dense sequence of dendrons (grafting route).[8] The second utilizes monomers already having dendrons, which are allowed to undergo polymerization (macromonomer route).[5a,9] We adopted the macromonomer route to avoid the intrinsic problems of the grafting, such as achieving complete coverage of the polymer backbone with dendrons, solubility of the polymer backbone during the second reaction (grafting reaction), and purifying the product from the reaction mixture.

In this paper, we report the synthesis and fundamental thermal, spectral, electrochemical, and electroluminescent properties of novel poly(*p*-phenylenevinylene)s with a metal-collecting site. Enhanced hole injection was realized just by the complexation with metal ions.

Experimental Section

Materials and Measurements. 3,5-Bis(*tert*-butylphenyl)-4-phenyltriazole (TAZ) was purchased from the H. W. Sands Corp., and poly(3,4-ethylenedioxythiophene) doped with a sulfonated polystyrene (PEDOT) was from the Bayer Corporation. The other chemicals were purchased from Aldrich, Tokyo Kasei Co., Ltd., and Kantoh Kagaku Co., Inc. (reagent grade) and used without further purification.

The NMR spectra were recorded using a JEOL JMN400 FT-NMR spectrometer (400 MHz) in $CDCl_3$ + TMS (internal standard) solution. The UV−vis spectra were recorded on a Shimadzu UV-3100PC spectrometer with a sealed quartz cell (optical path length: 1 cm). The molecular weight of the polymer was determined in THF using size exclusion chromatography (SEC) equipped with online refractive index (RI), light-scattering (LS), and viscometer detectors (Viscotek, Model302 TDA). The photoluminescence (PL) and electroluminescence (EL) spectra of the polymers were obtained using a spectrofluorometer (JASCO FP-6500). Differential scanning calorimetry (DSC) analysis of the polymer was performed under a nitrogen atmosphere with a Rigaku DSC8230. The cyclic voltammetry experiments were performed with a BAS-100 electrochemistry analyzer. All measurements were carried out at room temperature with a conventional three-electrode configuration consisting of a platinum working electrode, an auxiliary platinum electrode, and a nonaqueous $Ag/AgNO_3$ reference electrode. The cyclic voltammogram (CV) was obtained with a polymer film dip-coated on a Pt electrode. The solvent in all experiments was acetonitrile, and the supporting electrolyte was 0.1 M tetrabutylammonium tetrafluoroborate. All reported potentials are referenced to an external Fc^+/Fc and are not corrected for the junction potential.

EL Device Fabrications. Multilayered EL devices having the structure of ITO/PEDOT/DPA-PPV/(TAZ)/Alq/CsF/Al were fabricated by successively spin-coating PEDOT in water (40 nm) and the DPA-PPVs (30 nm) in chlorobenzene on an ITO-coated glass anode. TAZ (1 nm), Alq (50 nm), CsF (1 nm), and Al (100 nm) were successively vacuum-deposited on the top of DPA-PPV. The film thickness of the polymers was measured by a DEKTAK 3030 profilometer. The emitting area was 9 mm^2. The current−voltage characteristics were measured using an Advantest R6243 current/voltage unit. Luminance was measured with a Minolta LS-100 luminance meter in air at room temperature.

The polymer complex was prepared by the following method. To a solution of the polymer in chloroform was added a solution of $SnCl_2$ (1 wt % vs the polymer) in acetonitrile and evaporated to dryness to produce the polymer complex.

General Procedure for the Polymerization of DPA-Br_2 Gn by the Heck Reaction. To a solution of DPA-Br_2 Gn[10] in chloroform was added a solution of $Eu(OTf)_3$ in acetonitrile. This solution was evaporated to dryness to obtain the DPA-Br_2 Gn-europium complex. The DPA-Br_2 Gn-europium complex, dibromobenzene (if necessary), **1**, $Pd(OAc)_2$, and P(*o*-tol)$_3$ were dissolved in diisopropylamine and NMP and heated at 90 °C under N_2. To remove any remaining bromine end groups, styrene was added, and the mixture was allowed to react for an additional 24 h. The reaction mixture was poured into a large amount of methanol, and then a yellow-brown precipitate was collected by filtration and purified by Soxhlet extraction with methanol.

2a. The previous procedure was followed using DPA-Br_2 G1 (0.50 g, 1.21 mmol) in chloroform to which was added a solution of $Eu(OTf)_3$ (0.73 g, 1.21 mmol) in acetonitrile. The DPA-Br_2 G1-europium complex, *p*-dibromobenzene (0.86 g, 3.6 mmol), **1** (1.40 g, 4.80 mmol), $Pd(OAc)_2$ (0.03 g, 0.12 mmol), and P(*o*-tol)$_3$ (0.15 g, 0.48 mmol) were dissolved in diisopropylamine (0.42 mL, 3.0 mmol) and 30 mL NMP and heated at 90 °C under N_2 for 24 h. The purification above produced a 62% yield. ^{1}H NMR (400 MHz, $CDCl_3$, 30 °C, TMS standard, ppm): δ 2.30−0.87 (m, $-CH_2-$, 15H), 3.95−3.73 (broad, $-OCH_2-$, 5H), 7.46−7.15 (broad, vinyl proton and aromatic protons); ^{13}C NMR (100 MHz, $CDCl_3$, 30°, TMS standard, ppm): δ 173.45 (C=N).

3a. The previous procedure was followed using DPA-Br_2 G1 (0.50 g, 1.21 mmol) in chloroform to which was added a solution of $Eu(OTf)_3$ (0.73 g, 1.21 mmol) in acetonitrile. The DPA-Br_2 G1-europium complex, *p*-dibromobenzene (2.01 g, 8.5 mmol), **1** (2.80 g, 9.68 mmol), $Pd(OAc)_2$ (0.03 g, 0.12 mmol), and P(*o*-tol)$_3$ (0.15 g, 0.48 mmol) were dissolved in diisopropylamine (0.42 mL, 3.0 mmol) and 30 mL NMP and heated at 90 °C under N_2 for 24 h. The purification above produced a 68% yield. ^{1}H NMR (400 MHz, $CDCl_3$, 30 °C, TMS standard, ppm): δ 2.27−0.93 (m, $-CH_2-$, 15H), 3.98−3.90 (broad, $-OCH_2-$, 5H), 7.56−6.98 (broad, vinyl proton and aromatic protons); ^{13}C NMR (100 MHz, $CDCl_3$, 30 °C, TMS standard, ppm): δ 174.83 (C=N).

2b. The previous procedure was followed using DPA-Br_2 G2 (0.60 g, 0.78 mmol) in chloroform to which was added a solution of $Eu(OTf)_3$ (1.40 g, 2.34 mmol) in acetonitrile. The DPA-Br_2 G2-europium complex, *p*-dibromobenzene (0.46 g, 1.9 mmol), **1** (0.75 g, 2.6 mmol), $Pd(OAc)_2$ (0.015 g, 0.07 mmol), and P(*o*-tol)$_3$ (0.08 g, 0.26 mmol) were dissolved in diisopropylamine (0.21 mL, 1.5 mmol) and 15 mL NMP and heated at 90 °C under N_2 for 4 days. The purification above produced a 48% yield. ^{1}H NMR (400 MHz, $CDCl_3$, 30 °C, TMS standard, ppm): δ 2.27−0.93 (m, $-CH_2-$, 15H), 3.98−3.87 (broad, $-OCH_2-$, 5H), 7.75−6.80 (broad, vinyl proton and aromatic protons); ^{13}C NMR (100 MHz, $CDCl_3$, 30 °C, TMS standard, ppm): δ 168.61, 168.21, 167.56 (C=N).

3b. The previous procedure was followed using DPA-Br_2 G2 (0.50 g, 0.78 mmol) in chloroform to which was added a solution of $Eu(OTf)_3$ (1.16 g, 1.94 mmol) in acetonitrile. The DPA-Br_2 G2-europium complex, *p*-dibromobenzene (1.07 g, 4.55 mmol), **1** (1.50 g, 5.20 mmol), $Pd(OAc)_2$ (0.015 g, 0.07 mmol), and P(*o*-tol)$_3$ (0.08 g, 0.26 mmol) were dissolved in diisopropylamine (0.21 mL, 1.5 mmol) and 20 mL NMP and heated at 90 °C under N_2 for 7 days. The purification above produced a 58% yield. ^{1}H NMR (400 MHz, $CDCl_3$, 30 °C, TMS standard, ppm): δ 2.29−0.73 (m, $-CH_2-$, 15H), 3.99−3.90 (broad, $-OCH_2-$, 5H), 7.75−7.00 (broad, vinyl proton and aromatic protons); ^{13}C NMR (100 MHz, $CDCl_3$, 30 °C, TMS standard, ppm): δ 168.62, 168.19, 167.55 (C=N).

(7) Yin, R.; Zhu, Y.; Tomalia, D. A.; Ibuki, H. *J. Am. Chem. Soc.* **1998**, *120*, 2678.

(8) (a) Zubarev, E. R.; Stupp, S. I. *J. Am. Chem. Soc.* **2002**, *124*, 5762. (b) Liang, C. O.; Helms, B.; Hawker, C. J.; Fréchet, J. M. J. *Chem. Commun.* **2003**, 2524.

(9) (a) Karakaya, B.; Claussen, W.; Gessler, K.; Saenger, W.; Schlüter, A.-D. *J. Am. Chem. Soc.* **1997**, *119*, 3296. (b) Percec, V.; Ahn, C.-H.; Cho, W.-D.; Jamieson, A. M.; Kim, J.; Leman, T.; Schmidt, M.; Gerle, M.; Möller, M.; Prokhorova, S. A.; Sheiko, S. S.; Cheng, S. Z. D.; Zhang, A.; Ungar, G.; Yeardley, D. J. P. *J. Am. Chem. Soc.* **1998**, *120*, 8619. (c) Jahromi, S.; Coussens, B.; Meijerink, N.; Braam, A. W. M. *J. Am. Chem. Soc.* **1998**, *120*, 9753. (d) Sato, T.; Jiang, D.-L.; Aida, T. *J. Am. Chem. Soc.* **1999**, *121*, 10658. (e) Setayesh, S.; Grimsdale, A. C.; Weil, T.; Enkelmann, V.; Müllen, K.; Meghdadi, F.; List, E. J. W.; Leising, G. *J. Am. Chem. Soc.* **2001**, *123*, 946. (f) Marsitzky, D.; Vestberg, R.; Blainey, P.; Tang, B. T.; Hawker, C. J.; Carter, K. R. *J. Am. Chem. Soc.* **2001**, *123*, 6965. (g) Schenning, A. P. H. J.; Martin, R. E.; Ito, M.; Diederich, F.; Boudon, C.; Gisselbrechtb, J.-P.; Grossb, M. *Chem. Commun.* **1998**, 1013.

Scheme 1. Synthesis of DPA-PPVs[a]

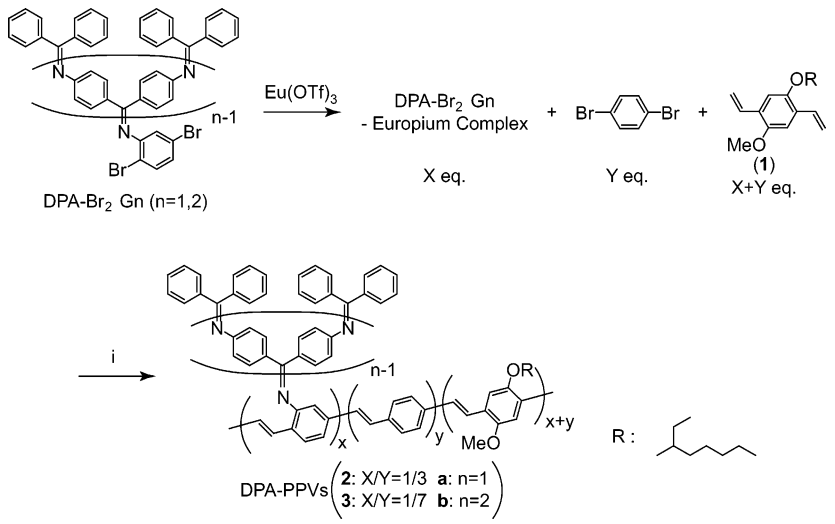

[a] Reagents and conditions: (i) (a) $Pd(OAc)_2$, P(*o*-tol)$_3$, (*i*-Pr)$_2$NH, NMP; (b) Styrene.

Table 1. Physical Properties of DPA-PPVs

	X/Y	yield (%)	*x/y*[a]	Mw[b]	Mw/Mn[b]	α[c]	T_g (°C)	λ_{max} (nm)[d]	λ_{em} (nm)[d]	λ_{PL} (nm)[e]	HOMO[f]/LUMO[g] (eV)
2a	1/3	62	1/3	13800	1.5	0.384	177	430	510	530	−5.16/−2.78
3a	1/7	68	1/8	37000	3.1	0.377	174	442	516	539	−5.07/−2.76
2b	1/3	48	1/7	26700	1.2	0.507	180	431	509	535	−5.12/−2.80
3b	1/7	58	1/16	23700	1.1	0.421	*h*	441	512	535	−5.06/−2.75

[a] Determined by profiling the amount of benzophenone produced via the hydrolysis reaction with sulfuric acid. [b] Determined using gel permeation chromatography equipped with a light-scattering detector in THF. [c] Mark−Houwink constant. [d] Measured in chloroform. [e] Film samples. [f] Estimated from the cyclic voltammetry. [g] Calculated from the absorption edge and the HOMO levels. [h] Not clearly observed.

Results and Discussion

Synthesis. The polymerization of the phenylazomethine monomers (DPA-Br_2) with 1-methoxy-4-(2-ethylhexyloxy)-2,5-divinylbenzene (**1**) was performed by the palladium-catalyzed Heck reaction as shown in Scheme 1.[10] We employed *p*-dibromobenzene as a spacer to reduce the ratio of DPA in the reaction mixture and the complexed macromonomers with $Eu(OTf)_3$ to avoid the deactivation of the palladium catalyst by complexation and filled the coordination trap site of the phenylazomethine for the catalyst.[11] The Heck reaction succeeded and yielded the corresponding polymer (DPA-PPV Gn) with higher molecular weights (MWs). $Eu(OTf)_3$ in the reaction mixture was removed by Soxhlet extraction. The DPA content in the polymer (*x/y*) was determined by profiling the amount of benzophenone produced via the hydrolysis of the polymers in the presence of sulfuric acid. These polymers are soluble in common organic solvents such as tetrahydrofuran (THF), chloroform, and toluene. The MWs of these polymers were determined using gel permeation chromatography equipped with online refractive index (RI), light-scattering (LS), and viscometer detectors as shown in Table 1. These results suggest that the steric hindrance between the DPA unit and **1** was reduced by introducing *p*-dibromobenzene as a spacer. Indeed, the polymerization profiles detected by preparative scale gel permeation chromatography (preparative GPC) revealed that the lower reaction rate of DPA-Br_2 G2 was estimated compared to that of DPA-Br_2 G1 on the basis of the degree of steric hindrance between the DPA unit and **1** (Figure 1). A longer reaction time was required for the reaction of DPA-Br_2 G2, while the reaction of DPA-Br_2 G1 finished within 1 day. DPA-Br_2 G2 could not be completely consumed, and for DPA-PPV G2, the DPA content in the polymer (*x/y*) was lower than the ratio of the monomers in the reaction mixture (*X/Y*).

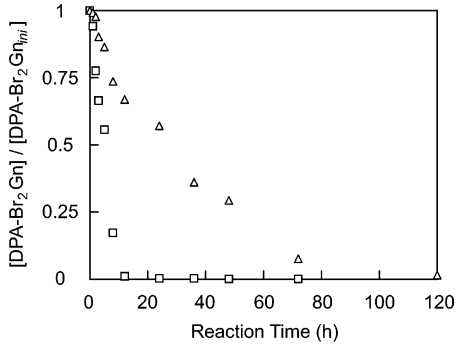

Figure 1. Reaction profile of DPA-Br_2 Gn with *X/Y* = 1/3; open square is $n = 1$ and open triangle is $n = 2$.

We directly observed the structure of DPA-PPV on the basis of the NMR spectra. The ^1H NMR spectra showed broad signals commonly monitored in polymeric materials. The vinylene peaks around 6.6 ppm attributed to the cis form could not be observed at all, whereas those of the trans form around 7.1 ppm were monitored although they overlapped the proton peak derived from the aromatic protons. The terminal vinyl peaks of **1** could be slightly seen at δ around 5.5 ppm. From the ^{13}C NMR spectra, the characteristic signals about 168 ppm assigned to the imine carbon were seen

(10) Kimoto, A.; Masachika, K.; Cho, J.-S.; Higuchi, M.; Yamamoto, K. *Org. Lett.* **2004**, *6*, 1179.

(11) Eu^{3+} ion was selected for the complexation with the phenylazomethine unit in the reaction because of the electrochemical stability.

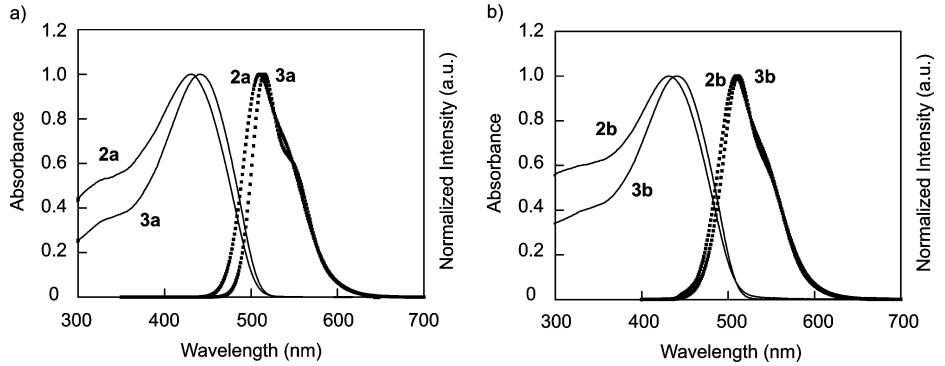

Figure 2. UV-vis (solid line) and fluorescence (dotted line)[13] spectrum of (a) DPA-PPV G1 and (b) DPA-PPV G2 in chloroform.

for all the DPA-PPVs. The number of imine peaks agree with that of our corresponding phenylazomethine dendrimers, for G1: one peak and G2: three peaks, different from those of DPA-Br_2 Gn, confirming evidence for introducing the DPA moiety in the polymer chain and not the mixture of the products of DPA-Br_2 Gn and PPVs derived from **1** and *p*-dibromobenzene.

Molecular Weights and Solution Properties. The solution property of the DPA-PPVs can be studied by SEC with triple detectors. The Mark−Houwink α exponent in THF at room temperature, which reflects the polymer chain conformation in the solution, estimated to be up to 0.5, indicated a large chain flexibility. Among them, DPA-PPV Gn with the lower dendron unit content (**3a** and **3b**) had a smaller Mark−Houwink α value than the DPA-PPVs with the higher dendron content (**2a** and **2b**), suggesting the smaller molecular density. As well, we compared **3a** and **2b**, which have DPA with almost the same content, suggesting the smaller molecular density with a small dendron unit confirmed by the smaller Mark−Houwink α value.

Thermal Properties. The thermal characterization of polymers was accomplished by differential scanning calorimetry (DSC). The glass transition temperature (T_g) of the polymers is also shown in Table 1. All the DPA-PPVs with higher T_g's than that of the MEH-PPV[12] suggested that the limited flexibility of the main chain was due to the introduction of the rigid substituent. Among the DPA-PPV G1s, **3a**, which contains a lower content of the dendron, shows a lower T_g with its smaller density, resulting in a high chain flexibility, supported by the Mark−Houwink results. We then compared **3a** and **2b**, having DPA with almost the same content, showing a higher T_g of **2b** with a larger molecular density with the dendron unit having a higher generation number supported by the higher Mark−Houwink α value.

Optical Properties. The UV−vis and fluorescent spectra of the polymer solution are shown and listed in Figure 2 and Table 1. As shown here, these polymers show an absorption band around 435 nm attributed to the $\pi-\pi^*$ transition of the main polymer chain, whereas DPA has an absorption band around 300−425 nm. The absorption at 400 nm, which mainly reflects the number of imine moieties ($n = 1$: one unit, $n = 2$: three unit) is in the following order: **3a** < **3b** < **2a** < **2b**, which agrees with the actual content of DPA estimated from the preparative GPC analyses. DPA-PPVs with the higher dendron content (**3a** and **3b**) have a longer λ_{max} value than polymers with a smaller ratio DPA (**2a** and **2b**), suggesting the influence of their electronic structure on the main chain by introducing the DPA unit. On the basis of this, a planar structure of PPV was followed by the introduction of DPA with a small degree. Also, compared with MEH−PPV that has a longer λ_{max}, a twisted polymer structure was formed by the induction of the bulky rigid dendron unit with the limited π delocalization. Indeed, the larger dendronized effect on the conjugation length was enclosed with DPA-PPVs of a larger generation, when compared between **3a** and **2b**. Attaching the larger rigid dendron into the PPV resulted in their coplanar structure and thus shorter λ_{max}. The same discussion can be applied to their fluorescent properties.

Metal-Collecting Properties. With the addition of $SnCl_2$ to the chloroform solution of the DPA-PPVs and their model compounds, 2,5-distyrylbenzene with the phenylazomethine dendron substituted at its 1-position (DPA-DSB Gn), the UV spectrum changed in a way similar to that of the model compounds, suggesting that the DPA group in the polymer is also capable of assembling metals (Figure 3). Among the complexation of DPA-DSB G1 and $SnCl_2$, the UV spectrum showed two unusual isosbestic nodes (367 and 417 nm) in the visible region (>300 nm), while only one isosbestic node was observed for the complexation of DPA-DSB G2 around 340 nm (Figure 3a and 3c). On the other hand, DPA-PPV G1 possesses two isosbestic nodes at 335 and 501 nm for **2a**, where DPA-PPV G2 shows one node around 360 nm for **2b** for the complexation of $SnCl_2$ with DPA (Figure 3b and 3d). These representive spectral changes similar to their model compounds indicate that the complexation of $SnCl_2$ could take place at their phenylazomethine unit beside the polymers.[6a, 6d,14] The isosbestic points of **2b** and **3b** were not clear because of a smaller change in the absorption and the lower absorption ratio attributed to DPA than that of PPV.[15]

Cyclic Voltammometric Studies. The electrochemical properties of the DPA-PPVs were studied by cyclic

(12) Kim, J. L.; Kim, J. K.; Cho, H. N.; Kim, D. Y.; Kim, C. Y.; Hong, S. I. *Macromolecules* **2000**, *33*, 5880.

(13) Excited at their absorption maximum, respectively.

(14) (a) Yamamoto, K.; Higuchi, M.; Shiki, S.; Tsuruta, M.; Chiba, H. *Nature* **2002**, *415*, 509. (b) Imaoka, T.; Horiguchi, H.; Yamamoto, K. *J. Am. Chem. Soc.* **2003**, *125*, 340. (c) Higuchi, M.; Tsuruta, M.; Chiba, H.; Shiki, S.; Yamamoto, K. *J. Am. Chem. Soc.* **2003**, *125*, 9988.

(15) We identified the number of metal ions by UV−vis spectroscopy. On the basis of the result, Sn^{2+} ions bind to all the binding sites. The number agreed with the imine units determined by the hydrolysis method.

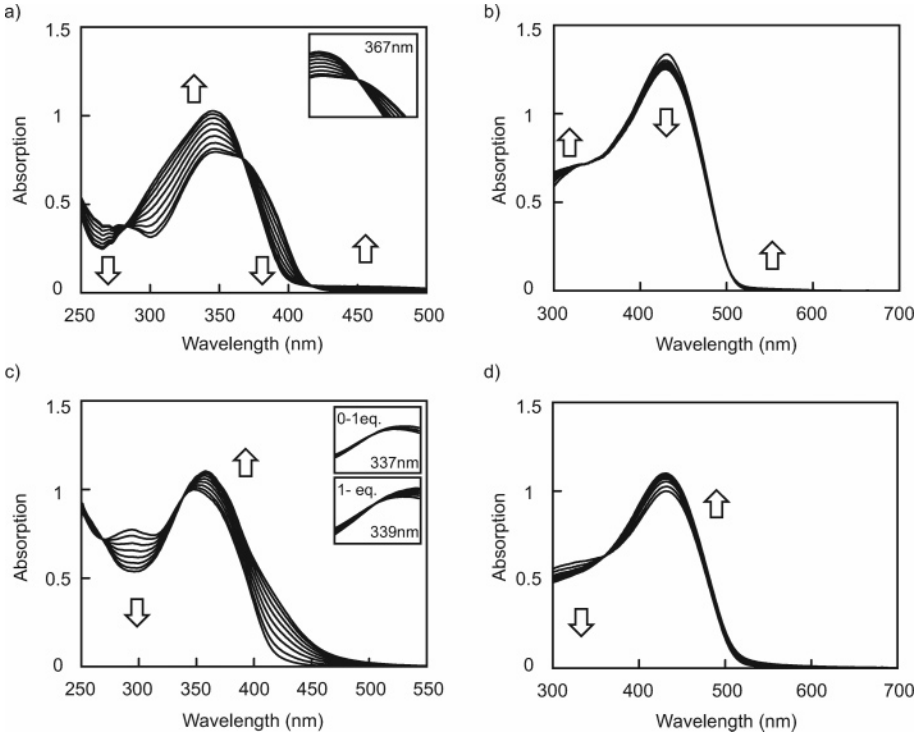

Figure 3. UV-vis spectra changes of (a) DPA-DSB G1, (b) **2a**, (c) DPA-DSB G2, and (d) **2b** upon the stepwise addition of $SnCl_2$ in the mixture of chloroform and acetonitrile. Insets show isosbestic points.

voltammetry. The cyclic voltammogram (CV) was obtained with a polymer film dip-coated on a Pt electrode in acetonitrile. Typically, during the cathodic and anodic scans, the DPA-PPVs show irreversible *n*- and *p*-doping processes. Using the cyclic voltammetry and UV−vis spectra,[16] we estimated the HOMO and LUMO energy levels, which hold the important parameters for an OLED configuration, especially where the recombination of holes and electrons takes place. The oxidation and reduction potentials are compared with the reduction potential of Fc/Fc^+. The band gap energy of DPA-PPVs was estimated from their absorption edge.[17] The HOMO energy level versus vacuum level was calculated from the measured onset potential of oxidation by comparison with ferrocene (4.8 eV below the vacuum level), and the LUMO energy level was calculated from the HOMO energy level and the absorption edge (Table 1).[18] The HOMO energy levels obtained here have a higher level with a lower content and a higher generation number of DPA; thus, **3b** has the highest HOMO level at −5.06 eV, while **2a** has the smallest at −5.16 eV. This difference in the HOMO energy level between G1 and G2 could be explained by the electronic state of their main chains induced by the electron density of the inner imines of DPA supported by the estimation of the coordination constants from the simulation of the titration curves and isosbestic points in our recent study.[14b] By complexing with $SnCl_2$, irreversible waves with almost the same potential for both the anodic and cathodic scans were observed as already reported. However, an additional stable redox wave attributed to the reduction of the azomethine-metal complex unit was not observed within the potential range.

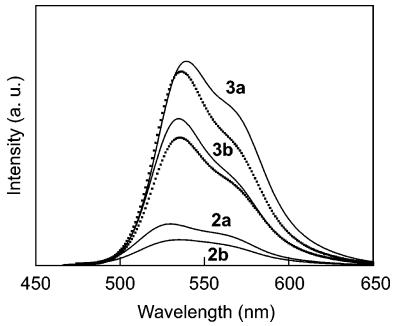

Figure 4. Photoluminescence spectrum of DPA-PPV (solid line, DPA-PPV; dashed line, DPA-PPV with $SnCl_2$ for **3a** and **3b**) excited at their maximum wavelength in the UV−vis absorption.

Photoluminescent Studies. Developed for OLEDs, the photoluminescent property of the emitting layer is essential for their characteristics with the relaxation efficiency by emitting light from its excited state. We investigated the photoluminescence spectra of DPA-PPVs. As shown in Figure 4, the photoluminescence intensity was reduced by increasing the ratio of the imine unit in DPA-PPV and the smallest photoluminescence was observed from **2b**, having the highest imine unit content in the polymer, while the lowest one, **3a,** showed the highest emission. This is due to the degree of energy transfer from PPV to DPA in the region between 400 and 500 nm, supported by the number of imine units in the polymer: **2b** > **2a** > **3b** > **3a**. The complexation with 1 wt % $SnCl_2$ did not drastically rely on their photoluminescence properties such as their spectra and intensity.

(16) (a) Wu, C.-C.; Strum, J. C.; Register, R. A.; Tian, J.; Dana, E. P.; Thompson, M. E. *IEEE Trans. Electron Devices* **1997**, *44*, 1269. (b) Kim, J. H.; Lee, H. *Chem. Mater.* **2002**, *14*, 2270.

(17) Janietz, S.; Bradley, D. D. C.; Grell, M.; Giebeler, C.; Inbasekaran, M.; Woo, E. P. *Appl. Phys. Lett.* **1998**, *73*, 2453.

(18) Kim, J. H.; Lee, H. *Chem. Mater.* **2002**, *14*, 2270.

(19) Kido, J.; Ohtaki, C.; Hongawa. K.; Okuyama, K.; Nagai, K. *Jpn. J. Appl. Phys.* **1993**, *32*, L917.

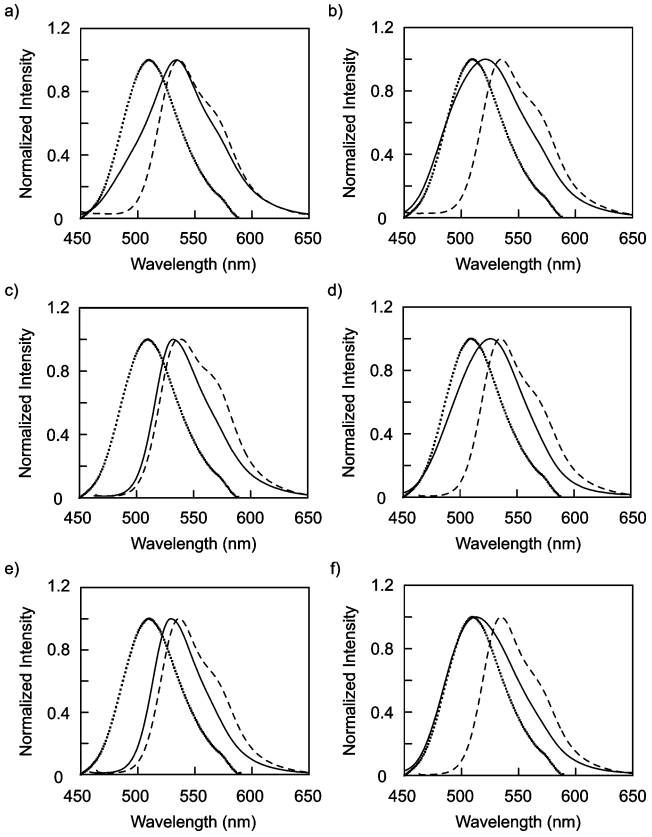

Figure 5. EL (solid line) and PL (dashed line) spectra of (a) type I with **3a**, (b) type I with **3b**, (c) type II with **3a**, (d) type II with **3b**, (e) type II with **3a** + $SnCl_2$, and (f) type II with **3b** + $SnCl_2$. The dotted line shows PL spectra of Alq.

Light-Emitting Diodes. Two types of EL devices were fabricated: (I) ITO/PEDOT/DPA-PPV/Alq/CsF/Al; (II) ITO/PEDOT/DPA-PPV/TAZ/Alq/CsF/Al, where Alq acts as an electron transport layer (ETL) and TAZ acts as a hole-blocking layer.[19] Bright green emissions were observed in all cases when a positive dc voltage was applied to the ITO electrode. In the type I devices without a hole-blocking layer, the photoluminescence spectra showed luminescence from both DPA-PPV and Alq (Figure 5a and b). This indicates that the electroluminescence originates from the recombination of holes and electrons injected into both Alq and DPA-PPV. Here, DPA-PPV acts not only as an emission layer but also as a hole-transporting layer. Above all, the maximum electroluminescence wavelength (λ_{EL}) is in the order **3a** (534 nm) > **3b** (523 nm) > **2a** = **2b** (505 nm) indicating the degree of emission from DPA-PPV, while Alq shows an emission band around 510 nm and the smallest maximum luminescence for the device was observed for **2b** (700 cd/m^2) (Figure 6a). The luminescence mainly from DPA-PPV was observed with a lower generation and a smaller amount of DPA (**3a**), on the basis of (1) their photoluminescence property, (2) HOMO energy levels, and (3) hole transport ability. The photoluminescent intensity actually lies in the order **3a** > **3b** > **2a** > **2b** corresponding to the number of imine units (Figure 4). The efficiency of the light emission by the recombination in the DPA-PPV layer could be reduced with more imine units. Also, the HOMO energy levels ($-5.06 \sim -5.16$ eV) of DPA-PPVs definitely lie between the cathode and Alq with relatively smaller (about 0.05 eV for generations) energy barriers at the DPA-PPV/Alq interface with the enhanced hole injection into the Alq layer. Comparing DPA-PPVs with a larger amount of DPA (**2a** and **2b**) as the emission layer, their drastic change in the electroluminescence characteristics did not agree with almost the same energy level. Thus, we should consider that the recombination ratio and the number of injected charges of DPA-PPV and Alq is almost the same for each.

In an attempt to obtain an emission from only DPA-PPV, TAZ, a hole-blocking layer, was introduced into the device (device II). In all cases, the emission from Alq was definitely, but not completely, reduced (Figure 5c and d). This suggests that the recombination at the Alq layer still exists and λ_{EL} is in the order **3a** > **3b** > **2b** > **2a**. This order with λ_{EL} is in accordance with device

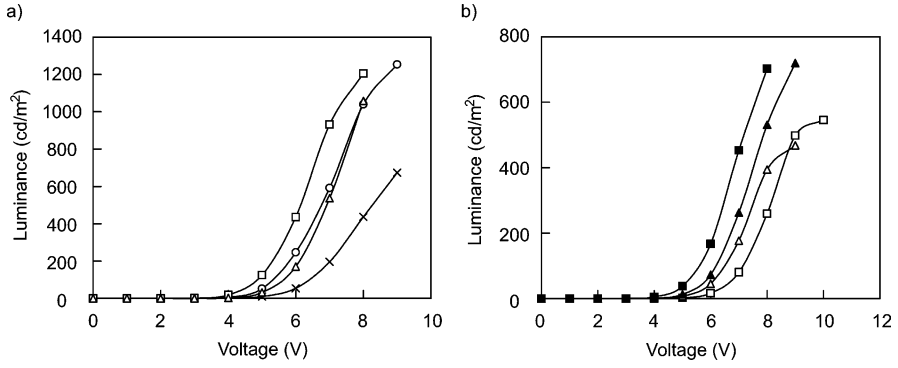

Figure 6. $L-V$ characteristics of OLEDs with the device (a) type I with circle, **2a**; cross, **2b**; square, **3a**; and triangle, **3b** and (b) type II with square, **3a**; triangle, **3b**, with open ones: DPA-PPV and closed ones: DPA-PPV with $SnCl_2$ complex.

Table 2. Electroluminescence Properties of DPA-PPVs[a]

	λ_{EL} (nm)	turn-on voltage (V)[b]	luminance (cd/ m^2)[c]	driving voltage (V)[d]	current density (mA/cm^2)[d]	η_{eff} (lm/W)[d]
3a	532	4.7	546	7.2	53	0.08
3a-$SnCl_2$	529	3.3	703	5.6	48	0.12
3b	527	4.3	468	6.5	38	0.13
3b-$SnCl_2$	513	4.0	720	6.5	27	0.19

[a] With the device structure of ITO/PEDOT/DPA-PPV/TAZ/Alq/CsF/Al. [b] Taken at a luminance of 0.1 cd/m^2. [c] At its maximum luminance. [d] Taken at a luminance of 100 cd/m^2.

I, suggesting no influence on their physical properties by introducing the TAZ layer in the device. As a result, a device with **3a** as an emission layer only shows luminescence from DPA-PPV itself (Figure 5c). On the other hand, no significant changes could be observed with a device containing **2a**, having the largest number of phenylazomethine units in the polymer. Considering that the recombination ratio is the same, the luminescence from Alq could be cut by the introduction of TAZ as well as **3a** with no relation to their photoluminescence properties. However, emission from Alq is actually observed, on the basis of the third discussion. We noticed the hole transport ability of the DPA moiety. We have already observed phenylazomethine oligomers themselves acting as a hole-transporting layer.[6b,6c] The number of imine units in DPA-PPV is in the following order: **3a** < **3b** < **2a** < **2b** in accordance with the degree of emission from Alq and this reflects the probability of functioning as a hole transporter. It is not certain whether the phenylazomethine unit directly acts as a hole transporter in the DPA-PPV unit.

For the type II device, the polymers with the low DPA content (**3a** and **3b**) complexes with a very small amount of $SnCl_2$ (1 wt %) films were then employed as an emitting layer. No significant change in the photoluminescent spectra was observed by the complexation with $SnCl_2$ because of the smaller spectral change in their absorption than in their fluorescence intensity (Figure 4, 5e, and 5f).

As shown in Figure 6b and Table 2, the low driving voltage and enhanced efficiency were followed by simple assembly of the metal ions. For the device with **3a**, the luminescence from DPA-PPV was successfully monitored (Figure 5e) and the turn-on voltage was reduced from 4.7 to 3.3 V and the maximum luminescence was enhanced from 546 cd/m^2 to 703 cd/m^2 by only complexing with a very small amount of $SnCl_2$. The threshold voltages for obtaining a luminance of 100 cd/m^2 were 7.2 and 5.6 V for the cells, respectively. Interestingly, for the device with **3b**, the emission from Alq was enhanced by the complexation (Figure 5f), indicating that recombination occurred and **3b**-$SnCl_2$ mainly acts as a hole transport layer. This is due to the enhanced hole injection and recombination into the Alq layer,[7] which could not be completely blocked on the basis of the enhanced hole transport property of the phenylazomethine unit by the TAZ layer. This result suggests that the luminescence property such as the recombination area of the device with DPA-PPVs essentially depends not on their photoluminescence property, but definitely on the hole transport ability of the phenylazomethine backbone.

Summary

In summary, we have synthesized and determined the physical properties of novel poly(*p*-phenylenevinylene)s (PPVs) possessing pendant phenylazomethine (DPA) dendrons. These polymers had solution, thermal, and optical properties affected by the content and generation of the DPA unit. DPA-PPV with the lower content and a smaller generation number had the longest absorption and fluorescence maximum wavelengths with a relatively planar structure and longer conjugation length. These polymers successfully assemble metal ions on their imine site supported by the spectral change similar to their monomeric model compounds. In two types of EL devices with (I) ITO/PEDOT/DPA-PPV/Alq/CsF/Al and (II) ITO/PEDOT/DPA-PPV/TAZ/Alq/CsF/Al, the luminescence from DPA-PPV was observed with a lower generation and a smaller amount of the DPA unit (**3a**), as explained by their HOMO energy levels and hole transport properties. For the device with **3a**, the low driving voltage and enhanced efficiency were obtained by simply complexing with a very small amount of $SnCl_2$.

Acknowledgment. This work was partially supported by CREST from the Japan Science and Technology Agency, Grants-in-Aid for Scientific Research (Nos. 15036262, 15655019, 15350073), and the 21st COE program (KEIO-LCC) from the Ministry of Education, Culture, Sports, Science, and Technology, and a Research Grant (Project No.23) from the Kanagawa Academy of Science and Technology.

Supporting Information Available: Additional spectroscopic data and cyclic voltammetric data (pdf). This material is available free of charge via the Internet at http://pubs.acs.org.

CM049241M